Journal of Biomechanics 84 (2019) 161–171

Contents lists available at ScienceDirect

Journal of Biomechanics

journal homepage: www.elsevier.com/locate/jbiomech
www.JBiomech.com

Hypersensitivity of trunk biomechanical model predictions to errors in image-based kinematics when using fully displacement-control techniques

A.H. Eskandari [a], N. Arjmand [a,*], A. Shirazi-Adl [b], F. Farahmand [a]

[a] Department of Mechanical Engineering, Sharif University of Technology, Tehran, Iran
[b] Division of Applied Mechanics, Department of Mechanical Engineering, Polytechnique, Montréal, Québec, Canada

ARTICLE INFO

Article history:
Accepted 28 December 2018

Keywords:
Spine
Finite element model
Musculoskeletal
Monte Carlo Method
Sensitivity

ABSTRACT

Recent advances in medical imaging techniques have allowed pure displacement-control trunk models to estimate spinal loads with no need to calculate muscle forces. Sensitivity of these models to the errors in post-imaging evaluation of displacements (reported to be ~0.4–0.9° and 0.2–0.3 mm in vertebral displacements) has not yet been investigated. A Monte Carlo analysis was therefore used to assess the sensitivity of results in both musculoskeletal (MS) and passive finite element (FE) spine models to errors in measured displacements. Six static activities in upright standing, flexed, and extended postures were initially simulated using a force-control hybrid MS-FE model. Computed vertebral displacements were subsequently used to drive two distinct fully displacement-control MS and FE models. Effects of alterations in the reference vertebral displacements (at 3 error levels with SD (standard deviation) = 0.1, 0.2, and 0.3 mm in input translations together with, respectively, 0.2, 0.4, and 0.6° in input rotations) were investigated on the model predictions. Results indicated that outputs of both models had substantial task-dependent sensitivities to errors in the measured vertebral translations. For instance, L5-S1 intradiscal pressures (IDPs) were considerably affected (SD values reaching 1.05 MPa) and axial compression and shear forces even reversed directions as translation errors increased to 0.3 mm. Outputs were however generally much less sensitive to errors in measured vertebral rotations. Accounting for the accuracies in image-based kinematics measurements, therefore, it is concluded that the current measured vertebral translation errors at and beyond 0.1 mm are too large to drive biomechanical models of the spine.

1. Introduction

Spine biomechanical models are diverse in terms of approach, objectives and application. In clinical biomechanics (e.g., implants design, investigation of failure and degenerative processes, development of effective preventive and rehabilitation programs) models are needed that provide sufficient details on the internal load sharing between different active (muscles) and passive (ligaments, facets, and discs) structures under various *in vivo* loading conditions. On the other hand, estimation of global mechanical loads on the intervertebral joints may be all that is required in occupational biomechanics and workplace ergonomics. Various biomechanical models with different degrees of complexity and accuracy have, therefore, been introduced.

Regardless of the biomechanical models employed, however, an intricate procedure to estimate unknown trunk muscle forces is a perquisite to a reliable calculation of intervertebral joint loads. This is because, joint loads are substantially affected by the forces in muscles that, due to their lever-arm disadvantage, often reach values much greater than the weights lifted in hands and/or the upper body-weight (Arjmand and Shirazi-Adl, 2005; Reeves and Cholewicki, 2003). Estimation of muscle forces in the trunk indeterminate system of equations is carried out based on a number of approaches, e.g., optimization, electromyography (EMG) or combination thereof using inverse or forward dynamics (Dreischarf et al., 2016). In a force-control model, muscle forces should verify measured kinematics and moment equilibrium requirements between external (gravity and inertial) and internal (passive and active) forces.

As an alternative to the traditional force-control trunk models, a number of purely displacement-control loading protocols (Dehghan Hamani et al., 2019; Wang et al., 2014; Zanjani-Pour

* Corresponding author at: Sharif University of Technology, Tehran 11155-9567, Iran.
E-mail address: arjmand@sharif.edu (N. Arjmand).

https://doi.org/10.1016/j.jbiomech.2018.12.043
0021-9290/

et al., 2018; Zanjani-Pour et al., 2016), in which intervertebral joint loads are estimated directly without muscle force calculations, have also emerged. By taking advantage of recent advances in the medical imaging tools and techniques, these models are driven by the measured *in vivo* displacements rather than the external, gravity and muscle forces. For instance, a subject-specific linear finite element (FE) model of the L3-L5 spine (with no facets) developed based on MR images (0.5 Tesla) in supine posture was driven by subject-specific fluoroscopy displacements to predict *in vivo* joint loads in 12 healthy subjects during upright, flexion and extension tasks (Zanjani-Pour et al., 2018). In another study, supine MR images (3.0 Tesla) were used to develop personalized L3-L4 disc finite element models (with no facets, ligaments, or vertebrae) of 3 subjects that were subsequently driven by endplate displacements recorded by dual fluoroscopy in static upright (flexed, neutral and extended) postures (Wang et al., 2014). We recently used subject-specific radiographic displacements to drive detailed nonlinear FE models of T12-L1 spine (with facets, ligaments, and vertebrae) of five subjects in static upright (flexed, neutral and extended) postures (Dehghan Hamani et al., 2019).

Although the partial validity of displacement-driven models has been demonstrated by comparing their predictions for intradiscal pressure (IDP) with the measured *in vivo* values under similar activities, their sensitivity to the inherent (imaging measurement and landmark identification) errors in post-imaging evaluation of displacements has not yet been investigated. Root-mean-square errors of ~1.6° and 2 mm in displacements have been reported when using fluoroscopic measurements of vertebral rotations and translations, respectively (Frobin et al., 1996; Pearcy et al., 1984). Recent studies, however, have reported considerably smaller errors of ~0.4–0.9° and 0.2–0.3 mm in MR- or CT-based measurements of vertebral displacements (Aiyangar et al., 2014; Ali et al., 2012; Dombrowski et al., 2018; Wang et al., 2014; Zanjani-Pour et al., 2016). These advances towards more accurate imaging techniques are encouraging in the field of biomechanical modeling especially in view of the higher sensitivity of spinal loads to prescribed segmental translations (Dehghan Hamani et al., 2019; Zanjani-Pour et al., 2016). In a study on the sensitivity of the contact characteristics computed in total knee replacements to errors in displacement measurements, substantial effects were found under rather small variations of ±0.1 mm or degree in input displacements (Fregly et al., 2008).

The present study therefore aims to use a Monte Carlo analysis to assess the sensitivity of results in two distinct fully displacement-control musculoskeletal (MS) and passive (FE) spine models to variations in measured displacements when simulating various static activities.

2. Methods

Our validated hybrid MS-FE model of the spine model is used to simulate six tasks.

2.1. MS model

Our previously-developed MS model evaluates forces in trunk muscles using an optimization algorithm along with equilibrium equations at all directions and T12-L5 vertebral levels. The pelvis, T1-T12 thorax and lumbar vertebrae are taken rigid (Fig. 1a and b). T12-L1 through L5-S1 motion segments are represented by 3-node nonlinear shear-deformable beams. The relaxed upright standing posture is constructed by applying optimal vertebral rotations (El-Rich et al., 2004) to the undeformed CT-based geometry. These rotations are determined while minimizing the sum of lumbar segmental moments generated by back muscles in the relaxed upright posture. Based on our earlier *in vivo* measurements for each task, the rotation of thorax (T), pelvis (P), and lumbar (L = T – P; partitioned between T12 to L5 vertebrae) as well as gravity/hand loads (Fig. 1a and b) are prescribed into the model of upright posture. To determine muscle forces, an optimization algorithm minimizing sum of cubed muscle stresses is used. Overall joint loads (local compression and shear loads at the beams) are subsequently calculated. The MS model has previously been validated by comparing its predicted muscle forces and compressive loads versus measured muscle EMG and IDPs, respectively (Arjmand et al., 2009, 2010).

2.2. Passive FE model

This model is constructed based on CT images of the T12-S1 lumbar spine of a cadaver (65 years-old male) (Breau et al., 1991; Khoddam-Khorasani et al., 2018; Shirazi-Adl, 1994b) (Fig. 1c and d). Seven vertebrae (T12 through S1 as rigid bodies), six discs (annulus and nucleus), 12 pairs of contact facet surfaces, and nine sets of ligaments are included. The geometry of the spine (dimensions and lumbar lordosis) in the MS and FE models is identical. Annulus layers and disc nucleuses are represented as, respectively, isotropic annulus bulk (reinforced by membranes of collagen fibres) and fluid-filled cavities. Hyperelastic Mooney-Rivlin material properties ($c_1 = 0.42$, $c_2 = 0.105$) are used for the ground substance of the annulus bulk. 14 distinct collagen fiber layers are represented using membrane layers reinforced by rebar elements (with criss-cross patterns at ±30° and nonlinear stress-strain data for material properties (Shirazi-Adl et al., 1984)) distributed in the foregoing annulus ground substance. Facet articulations are simulated by frictionless surface-to-surface contacts with gap limit of 1.25 mm set to initiate articulation (simulating compliant articular cartilage layers). Ligaments (Fig. 1c and d) are modeled by multiple axial tension-only elements with nonlinear properties. Each nucleus region at the disc center within annulus layers is simulated as an incompressible fluid-filled cavity. The passive FE model has previously been validated by comparing its predicted range of motion (RoM), IDP, facet joint forces (FJFs) under pure moment loading, pure compressive loading, and a combination thereof versus measured in vitro and *in vivo* data (Khoddam-Khorasani et al., 2018).

2.3. Force-control hybrid model to set reference results

For each task, the associated pelvic rotation measured *in vivo* and muscle forces estimated in the MS model (via connector elements) are prescribed into the passive FE model. Each uniaxial connector element runs between a muscle upper and lower insertion points. The force-elongation relation of each connector element is defined as a step-function so that it yields an axial force identical to that already computed in the MS model regardless of the elongation in the connector element. In addition, gravity loads and weight in hands are applied at their locations measured *in vivo*. Despite identical loading conditions, slightly different deformed configurations (between MS and passive FE models) are computed due to distinct simulations (e.g., compression-dependent stiffness) of motion segments. To ensure identical final deformed T12-S1 kinematics between the MS and FE models, the analysis of MS model is repeated after adjustments in its passive, compression-dependent stiffness (moment-rotation) properties based on those in the passive FE model under identical gravity loads, weight held in hands and muscle exertions. The updated muscle forces are again prescribed into the passive FE model and this iterative procedure is continued until convergence, i.e., the two models reach almost identical kinematics for the simulated task (average difference of <1 mm between the MS and FE models for the final global

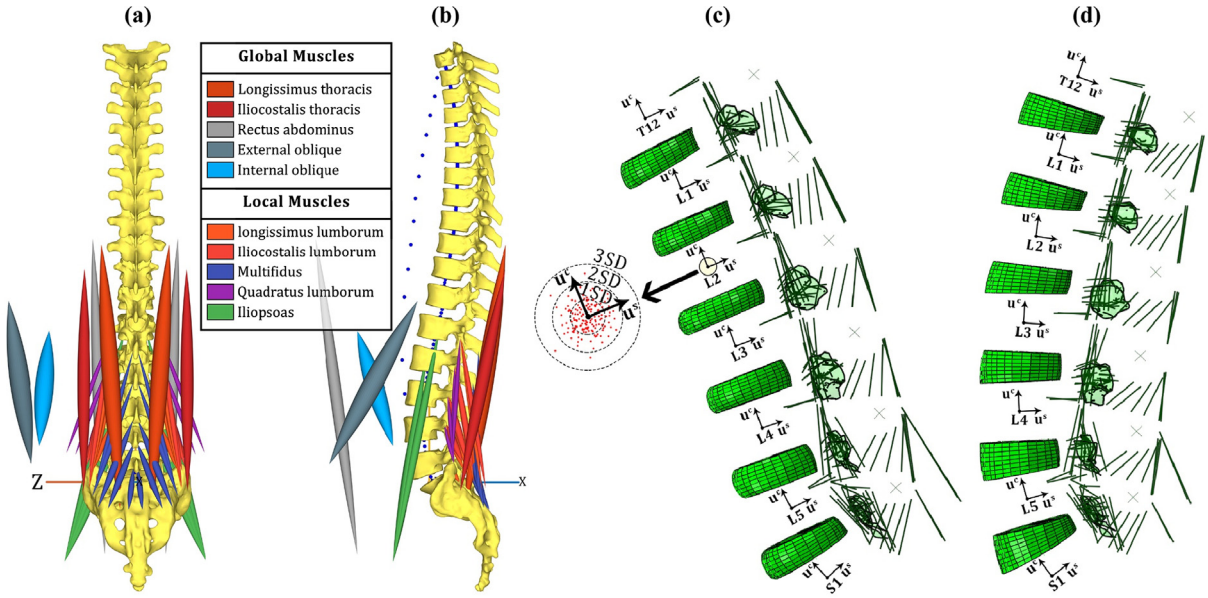

Fig. 1. (Left) Musculoskeletal (MS) model as well as representation of global and local musculatures in the frontal (back view) (a) and sagittal (b) planes. The trunk weight of ~344 N (~52% of the total body weight of a male subject in our earlier studies with a body mass of ~68 kg) is partitioned among upper arms (~36 N), forearms/hands (~29 N), head (46 N) (applied on the rigid thorax via rigid elements at their mass centers as recorded in our *in vivo* measurements), and T1-L5 segments as shown by solid dots (~233 N between the T1 through L5 segments and applied via rigid elements at their mass centers located anteriorly at each vertebra). For tasks with a hand load, a force in the gravity direction was also applied via a rigid element attached to the rigid thorax at the T3 at a location measured *in vivo*. In total, 56 muscles are incorporated. Curved lines of action for global thoracic back muscles (i.e., their wrapping around and contact forces at bony vertebrae) are considered. (Right) Detailed finite element (FE) model in deformed (c) and undeformed (d) configurations. Included ligaments are anterior longitudinal (ALL), posterior longitudinal (PLL), capsular (CL), intertransverse (ITL), ligamentum flavum (LF), supraspinous (SSL), interspinous (ISL), fascia (L4 and L5 to ilium) and iliolumbar (IL, L5 to ilium) ligaments. Vertebral anterior and posterior bony bodies are simulated by distinct rigid elements attached together via two deformable beams at their respective pedicle centers. An example of normal distribution (SD: standard deviation) of displacements in the local coordinate system around the computed reference solution at the L2 vertebral body is also depicted. Crosses denote the primary nodes of the rigid bodies representing vertebral posterior bony structures.

positions of the T12-S1 vertebral centroids). In all simulations, the S1 translational degrees-of-freedom are constrained, pelvis rotation is prescribed based on measurements while remaining rotational and translational degrees-of-freedom at the vertebral levels are left unconstrained (i.e., predicted by the hybrid model).

T12-S1 IDPs, ligament forces, and FJFs are computed for each simulated task. Moreover, based on the free body diagrams at the disc mid-height planes, overall joint compression and shear forces are also determined in each activity. Sagittal translations and rotations of T12-S1 vertebral centers under the final converged config-

Table 1
Standard deviation and coefficient of variation, SD (CV), of model response variables (intradiscal pressure (IDP), compression, and shear) in different tasks and discs in the FE model.

	Sensitivity Analysis	Disc	Relaxed upright	Flex 20°	Flex 40°	Flex 60°	Flex 80°	Load handling
IDP (MPa)	Reference	L4-L5	0.45	0.80	1.23	1.56	2.00	0.93
		L5-S1	0.49	0.87	1.34	1.78	2.27	1.17
	0.1 mm & 0.2°	L4-L5	0.14 (30%)	0.18 (23%)	0.19 (15%)	0.21 (13%)	0.25 (12%)	0.16 (18%)
	SD (CV%)	L5-S1	0.18 (34%)	0.22 (25%)	0.23 (17%)	0.29 (16%)	0.32 (14%)	0.26 (22%)
	0.2 mm & 0.4°	L4-L5	0.29 (53%)	0.39 (44%)	0.36 (29%)	0.46 (29%)	0.50 (25%)	0.35 (36%)
	SD (CV%)	L5-S1	0.34 (62%)	0.42 (44%)	0.56 (41%)	0.65 (35%)	0.71 (31%)	0.50 (39%)
	0.3 mm & 0.6°	L4-L5	0.42 (77%)	0.51 (59%)	0.64 (47%)	0.65 (39%)	0.68 (33%)	0.52 (51%)
	SD (CV%)	L5-S1	0.47 (78%)	0.68 (65%)	0.77 (53%)	0.98 (50%)	1.05 (43%)	0.82 (61%)
Compression (N)	Reference	L4-L5	550	911	1280	1367	1713	1528
		L5-S1	632	1045	1489	1488	1856	1698
	0.1 mm & 0.2°	L4-L5	154 (28%)	206 (23%)	228 (18%)	275 (20%)	341 (20%)	227 (15%)
	SD (CV%)	L5-S1	238 (35%)	307 (28%)	330 (22%)	455 (31%)	527 (29%)	367 (21%)
	0.2 mm & 0.4°	L4-L5	326 (51%)	458 (45%)	447 (34%)	598 (44%)	685 (40%)	494 (30%)
	SD (CV%)	L5-S1	457 (66%)	582 (51%)	805 (53%)	1021 (64%)	1150 (61%)	712 (38%)
	0.3 mm & 0.6°	L4-L5	490 (75%)	606 (62%)	795 (56%)	863 (58%)	938 (53%)	756 (44%)
	SD (CV%)	L5-S1	647 (87%)	954 (75%)	1110 (69%)	1538 (89%)	1710 (82%)	1205 (61%)
Shear (N)	Reference	L4-L5	58	130	180	208	193	225
		L5-S1	195	323	408	377	376	596
	0.1 mm & 0.2°	L4-L5	35 (64%)	34 (28%)	38 (21%)	61 (28%)	60 (29%)	53 (23%)
	SD (CV%)	L5-S1	70 (35%)	77 (24%)	91 (22%)	94 (25%)	91 (25%)	99 (17%)
	0.2 mm & 0.4°	L4-L5	64 (115%)	79 (66%)	86 (45%)	115 (50%)	123 (55%)	98 (46%)
	SD (CV%)	L5-S1	122 (60%)	157 (46%)	163 (40%)	179 (51%)	176 (48%)	206 (33%)
	0.3 mm & 0.6°	L4-L5	97 (189%)	111 (104%)	131 (78%)	153 (67%)	176 (86%)	161 (74%)
	SD (CV%)	L5-S1	170 (76%)	215 (66%)	242 (58%)	236 (66%)	246 (68%)	324 (47%)

Table 2
Standard deviation and coefficient of variation, SD (CV), of model response variables (compression and shear forces) in different tasks and discs in the MS model.

	Sensitivity Analysis	Disc	Relaxed upright	Flex 20°	Flex 40°	Flex 60°	Flex 80°	Load handling
Compression (N)	Reference	L4-L5	451	911	1281	1401	1709	1529
		L5-S1	601	1045	1489	1409	1850	1698
	0.1 mm & 0.2°	L4-L5	387 (74%)	618 (63%)	648 (48%)	748 (49%)	691 (40%)	808 (49%)
	SD (CV%)	L5-S1	425 (65%)	564 (50%)	641 (40%)	627 (43%)	618 (32%)	661 (39%)
	0.2 mm & 0.4°	L4-L5	1081 (140%)	1195 (94%)	1399 (86%)	1328 (74%)	1200 (64%)	1466 (77%)
	SD (CV%)	L5-S1	940 (115%)	1077 (90%)	1281 (77%)	1150 (74%)	1165 (59%)	1540 (82%)
	0.3 mm & 0.6°	L4-L5	1618 (148%)	1775 (120%)	1742 (107%)	1631 (103%)	1514 (93%)	1831 (99%)
	SD (CV%)	L5-S1	1550 (149%)	1665 (115%)	1735 (93%)	1491 (87%)	1644 (71%)	2082 (91%)
Shear (N)	Reference	L4-L5	24	126	188	218	224	222
		L5-S1	117	328	426	396	411	589
	0.1 mm & 0.2°	L4-L5	66 (271%)	62 (49%)	65 (34%)	62 (29%)	61 (27%)	52 (23%)
	SD (CV%)	L5-S1	92 (78%)	86 (26%)	82 (19%)	79 (20%)	76 (18%)	62 (10%)
	0.2 mm & 0.4°	L4-L5	130 (633%)	123 (87%)	117 (66%)	107 (53%)	132 (61%)	97 (47%)
	SD (CV%)	L5-S1	192 (127%)	170 (54%)	154 (35%)	160 (39%)	159 (40%)	124 (21%)
	0.3 mm & 0.6°	L4-L5	192 (544%)	181 (159%)	187 (106%)	168 (77%)	185 (102%)	170 (74%)
	SD (CV%)	L5-S1	280 (206%)	238 (66%)	208 (46%)	244 (63%)	217 (49%)	191 (32%)

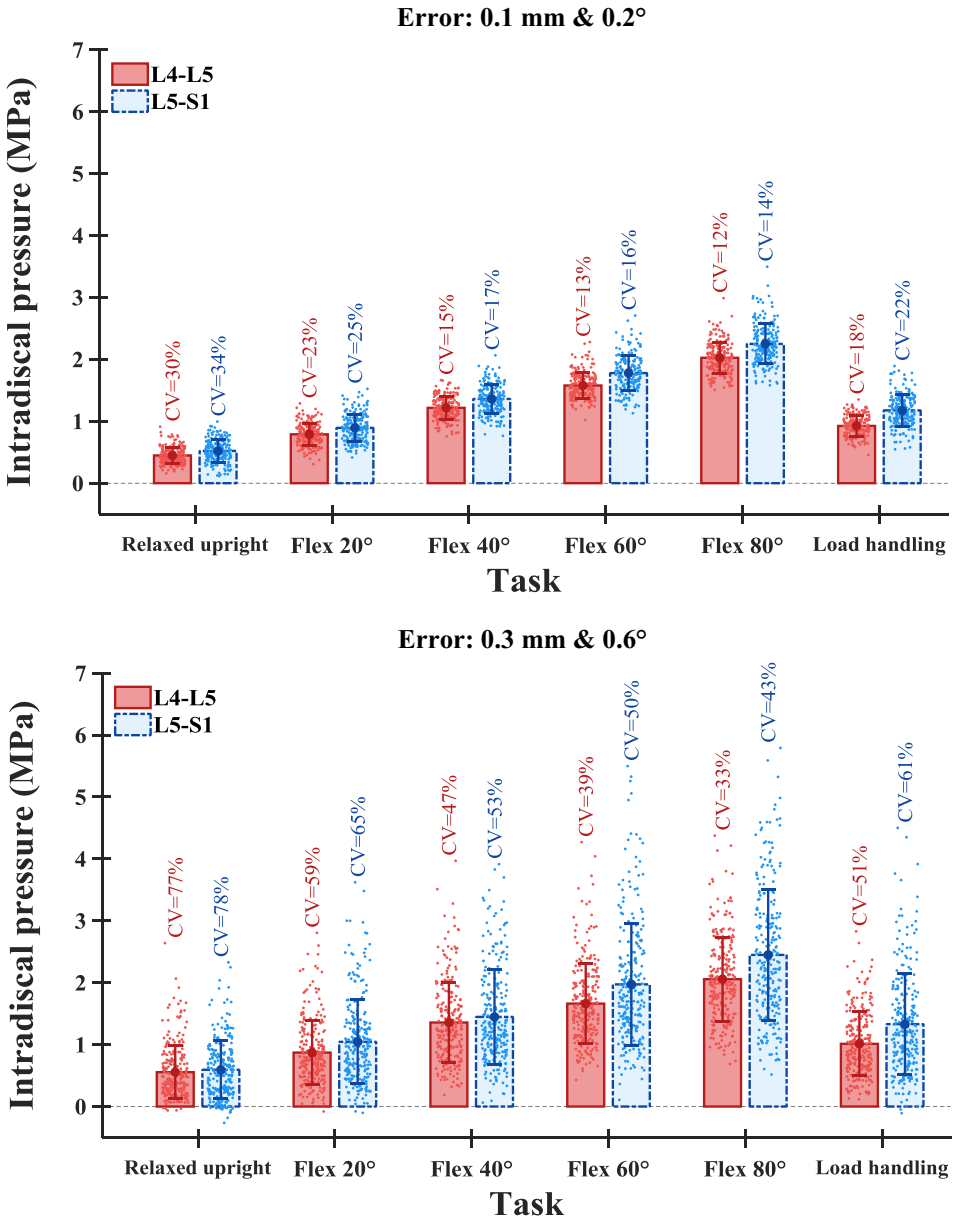

Fig. 2. Mean, standard deviation and coefficient of variation (CV) for the L4-L5 and L5-S1 intradiscal pressures (IDP) computed in the FE model in different tasks. The scatter dots (200 data points in each task) present the predicted IDPs for various sensitivity simulations (0.1 mm & 0.2° and 0.3 mm & 0.6°).

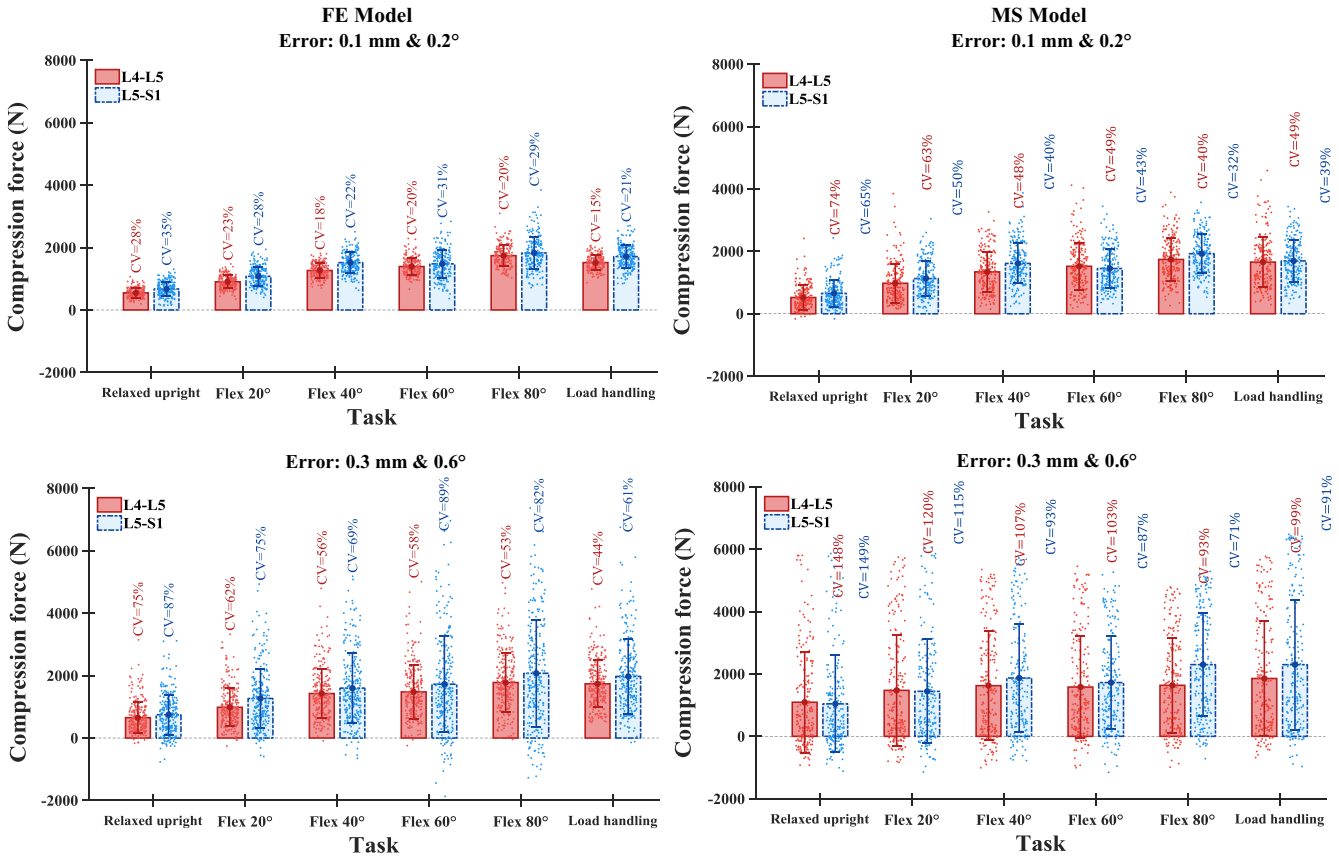

Fig. 3. Mean, standard deviation and coefficient of variation (CV) for the L4-L5 and L5-S1 compression forces computed in the FE (left) and MS (right) models in different tasks. The scatter dots (200 data points for each task) present the predicted compression forces for various sensitivity simulations (0.1 mm & 0.2° and 0.3 mm & 0.6°).

uration with respect to the upright standing posture (taken subsequently as reference displacement values) are subsequently calculated in MS and FE models (supplementary material 1). The hybrid model has previously been validated by comparing its predicted L4-L5 IDP in each task and L1-S1 CoRs in flexion tasks with available *in vivo* data (Khoddam-Khorasani et al., 2018).

2.4. Simulated tasks

Six symmetric static tasks including a neutral upright standing posture, forward flexions of 20, 40, 60, and 80° with arms in the gravity direction, and an upright two-handed lift of 19.8 kg at 25 cm anterior distance to the L5-S1 disc are considered.

2.5. Displacement-Control MS and FE models

For each simulated task, the calculated displacements (reference kinematics taken as the final sagittal translations and rotations at all vertebral levels in the force-control hybrid model) are separately applied into the MS and FE models while removing all externally-applied forces from these models. That is, each model (MS and FE) is driven by the displacements obtained from its corresponding force-control model. This results in fully displacement-control MS and FE models driven with identical kinematics as those of the force-control hybrid models. As to the FE model, the kinematics are prescribed only at the centroid of anterior vertebral rigid bodies while allowing the posterior bony elements to translate and rotate relative to their anterior bodies. Out-of-sagittal plane degrees-of-freedom are considered in both the MS and FE displacement-control models based on the displacements from their corresponding force-control models. Sensitivity analyses are, therefore, performed only on the sagittal plane displacements.

2.6. Monte Carlo sensitivity analysis

In order to investigate the sensitivity of the foregoing displacement-control MS and FE models, taken as the reference conditions, to the errors in the input sagittal translations and rotations, Monte Carlo sensitivity analyses are carried out. Unlike traditional sensitivity analyses (Fregly et al., 2008; Zanjani-Pour et al., 2016), the Monte Carlo technique assesses also the effect of possible interactions between input parameters on model outputs. For this, domain of variations in each vertebral displacement (about its reference value) is randomly sampled from the probability distribution in its local coordinate system (u^c, u^s, and u^r as in Fig. 1c and d). That is, normal distributions in input variations with standard deviations (SD) of 0.1, 0.2, and 0.3 mm for vertebral translations and of 0.2, 0.4, and 0.6° for vertebral rotations are prescribed on top of the already computed reference displacements of each vertebra. Two hundred sample sets for 21 local displacement parameters (two local sagittal translations and one sagittal rotation for T12 to S1 vertebrae) are generated (further sampling did not affect the predicted mean and variance of the response variables). Simulations are subsequently performed by each set of displacements in the displacement-control models and results are predicted. IDP, overall L4-S1 compression and shear loads, FJFs, and forces in L4-S1 ligaments are calculated in the FE model whereas overall L4-S1 compression and shear loads are calculated in the MS model. Mean, standard deviation (SD), and coefficient of variation (CV showing the relative extent of variation to the mean) for each output are subsequently calculated in each task. Pearson's

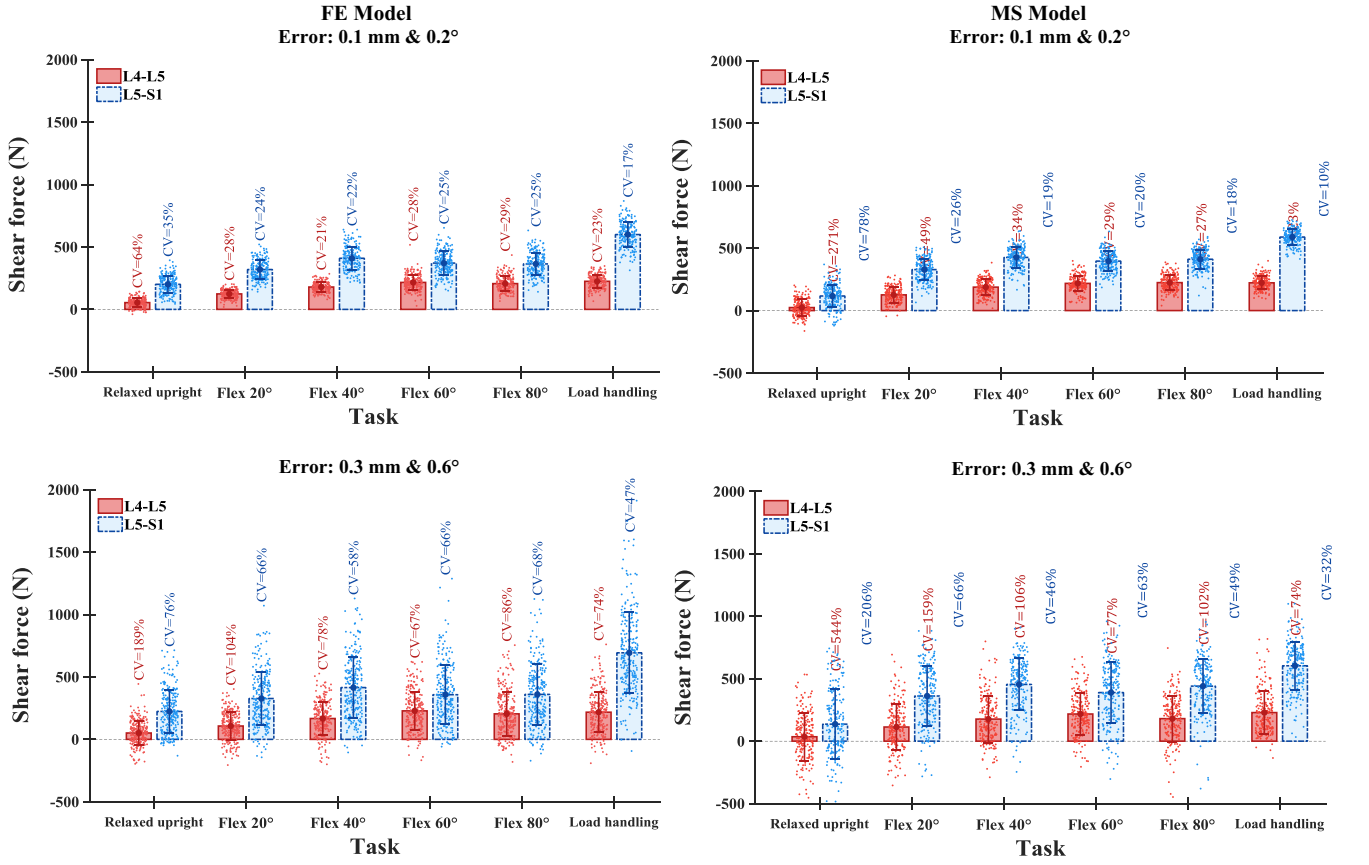

Fig. 4. Mean, standard deviation and coefficient of variation (CV) for the L4-L5 and L5-S1 shear forces computed in the FE (left) and MS (right) models in different tasks. The scatter dots (200 data points for each task) present the predicted shear forces for various sensitivity simulations (0.1 mm & 0.2° and 0.3 mm & 0.6°). Positive values indicate anterior shear force.

product-moment correlation coefficients between inputs (u^c, u^s, and u^r in Fig. 1c and d) and select outputs are also calculated to assess sensitivity of each model outputs to its inputs.

3. Results

Although sensitivity analyses were performed at all lumbar levels of both MS and FE models, results are presented here only for the lowermost L4-L5 and L5-S1 levels where compression and shear forces peak. Results of the force-control reference models at all levels are available elsewhere (Khoddam-Khorasani et al., 2018).

3.1. General findings

Predicted compression and shear forces in the reference force-control MS and FE models were similar with average differences for all tasks remaining smaller than 21 N (Tables 1 and 2). Regardless of the simulated task, changes in outputs in both FE and MS models increased as the errors in measured displacements increased from 0.1 mm and 0.2°, respectively, to 0.3 mm and 0.6° (Tables 1 and 2 and Figs. 2–6). Pearson correlation coefficient between input (local axial and shear translations as well as sagittal rotation) and select output (response) variables in different tasks indicated that the FE and MS model outputs were generally more sensitive to errors in the applied translations as compared to the applied sagittal rotations (see Figs. 7–8 for upright posture and supplementary materials 2 and 3 for flexion 80°). The only exception was the ligament forces in the FE model that were more sensitive to variations in the applied rotations. In general, ligament forces were the least and IDP/compression forces were the most sensitive outputs to alterations in input variables (Figs. 7 and 8 and supplementary materials 2 and 3). Moreover, the two models (MS and FE) had different sensitivities to input (displacement) errors (Tables 1 and 2 and Figs. 3 and 4). The predicted compression and shear forces by the MS model showed considerably larger SD and CV values as compared to those predicted by the FE model especially in the less demanding tasks (Tables 1 and 2).

3.2. FE model

L4-L5 and L5-S1 IDPs moderately varied (CVs $\leq$ 34% and SDs $\leq$ 0.32 MPa in all tasks) at lower displacement errors of 0.1 mm and 0.2° (Table 1 and Fig. 2). IDPs were, however, considerably affected (CV and SD values reaching 78% and 1.05 MPa, respectively) as displacement errors increased to 0.3 mm and 0.6°. Among the simulated tasks, the largest SD and CV values occurred in flexion 80° and relaxed upright posture, respectively. For instance, as displacement errors increased from 0.1 mm and 0.2° to 0.3 mm and 0.6°, the SD of L4-L5 and L5-S1 IDPs increased to, respectively, 0.68 and 1.05 MPa in the flexion 80° while corresponding CVs rose to 77% and 78% in the upright relaxed posture. Similar trends were found for the predicted joint compression forces (Table 1 and Fig. 3). Predicted shear forces were found significantly sensitive to the displacement errors; CV and SD values of 64% and 99 N, respectively at lower errors of 0.1 mm and 0.2° and of 189% and 324 N at greater errors of 0.3 mm and 0.6° (Table 1 and Fig. 4). Sensitivity of the predicted ligament forces to displacement errors was relatively small in all tasks (SD $\leq$ 37 N) but the

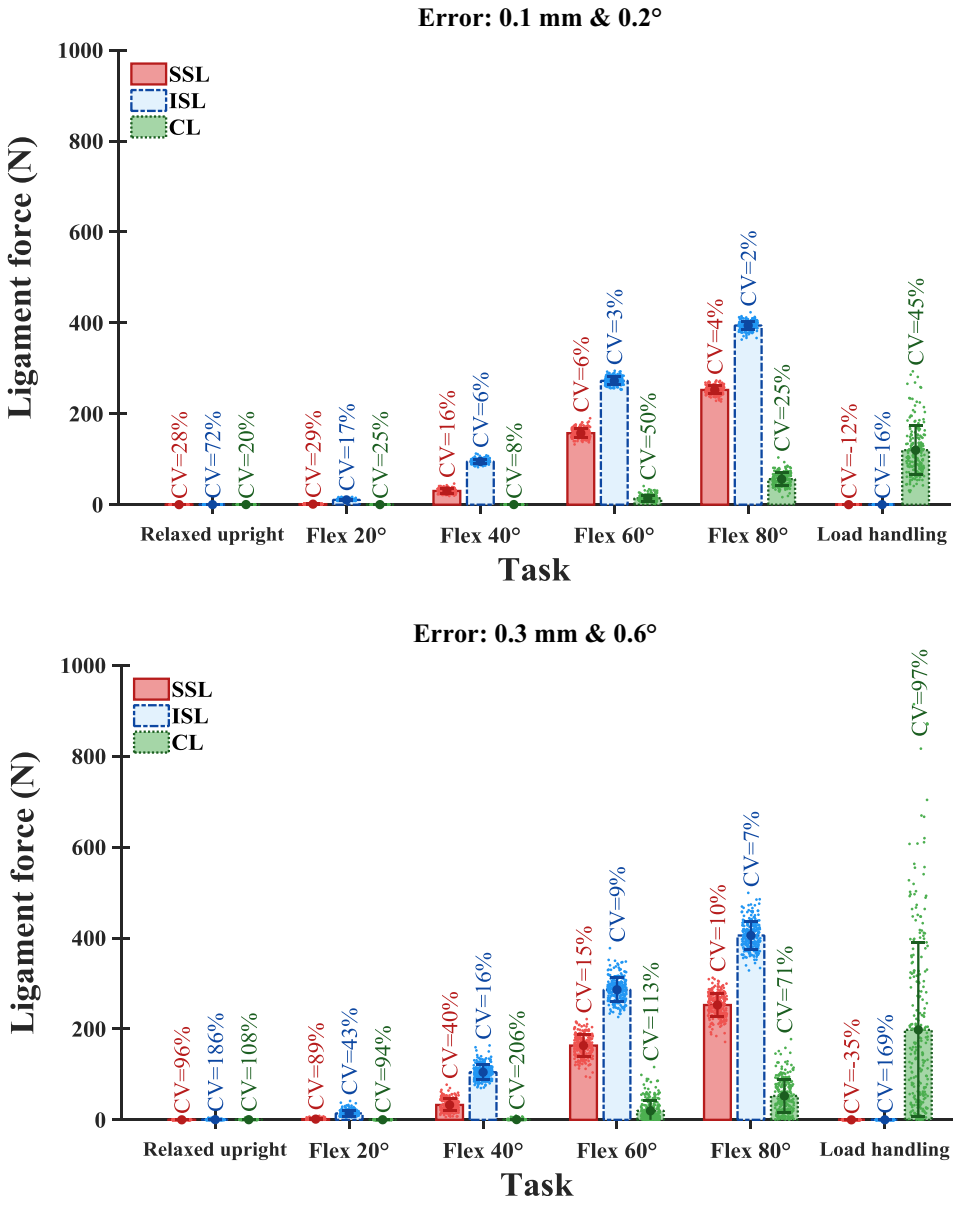

Fig. 5. Mean, standard deviation and coefficient of variation (CV) for the ligament forces in the L4-L5 motion segment (CL: capsular ligaments, SSL: Supraspinous ligaments, ISL: Interspinous ligaments) computed in the FE model in different tasks. The scatter dots (200 data points for each task) present the predicted ligament forces for various sensitivity simulations (0.1 mm & 0.2° and 0.3 mm & 0.6°).

load handling one in which maximal SD reached ~200 N (Fig. 5). On the other hand, displacement errors had significant effects on the predicted FJFs (Fig. 6); maximal SD value of 71 N for errors of 0.1 mm and 0.2° and of 258 N for errors of 0.3 mm and 0.6°. There were moderate to strong linear correlation between L4-L5 and L5-S1 IDP/compression forces and local axial translations, i.e. translations perpendicular to disc endplates ($|r| > 0.62$). Similarly, moderate to strong correlations between the shear force in those discs and local shear translations along the disc endplates were found ($|r| > 0.52$). Vertebral rotations had very weak correlation with IDP/compression ($|r| < 0.2$), moderately weak with shear response variables, and higher correlation with ligament forces (e.g. $|r|$ up to 0.8 for ISL).

3.3. MS model

Among the simulated tasks, the largest SD and CV values for the predicted compression forces occurred in upright tasks without and with load in hands, respectively. As for the shear forces, the largest SD and CV values both occurred in the former relaxed upright posture. Estimated compression and shear forces showed much greater sensitivity in the MS model than the FE model (Tables 1 and 2). There was moderate linear correlation between L4-L5 and L5-S1 compression and shear forces with, respectively, local axial ($0.47 < |r| < 0.7$) and shear translations ($0.24 < |r| < 0.63$).

4. Discussion

Outputs of both MS and FE models had generally substantial task-dependant sensitivities to errors in the measured vertebral translations. Outputs were however generally much less sensitive to errors in the measured vertebral rotations. Accounting for the accuracies in image-based kinematics measurements, therefore, it is concluded that measured vertebral translations are currently

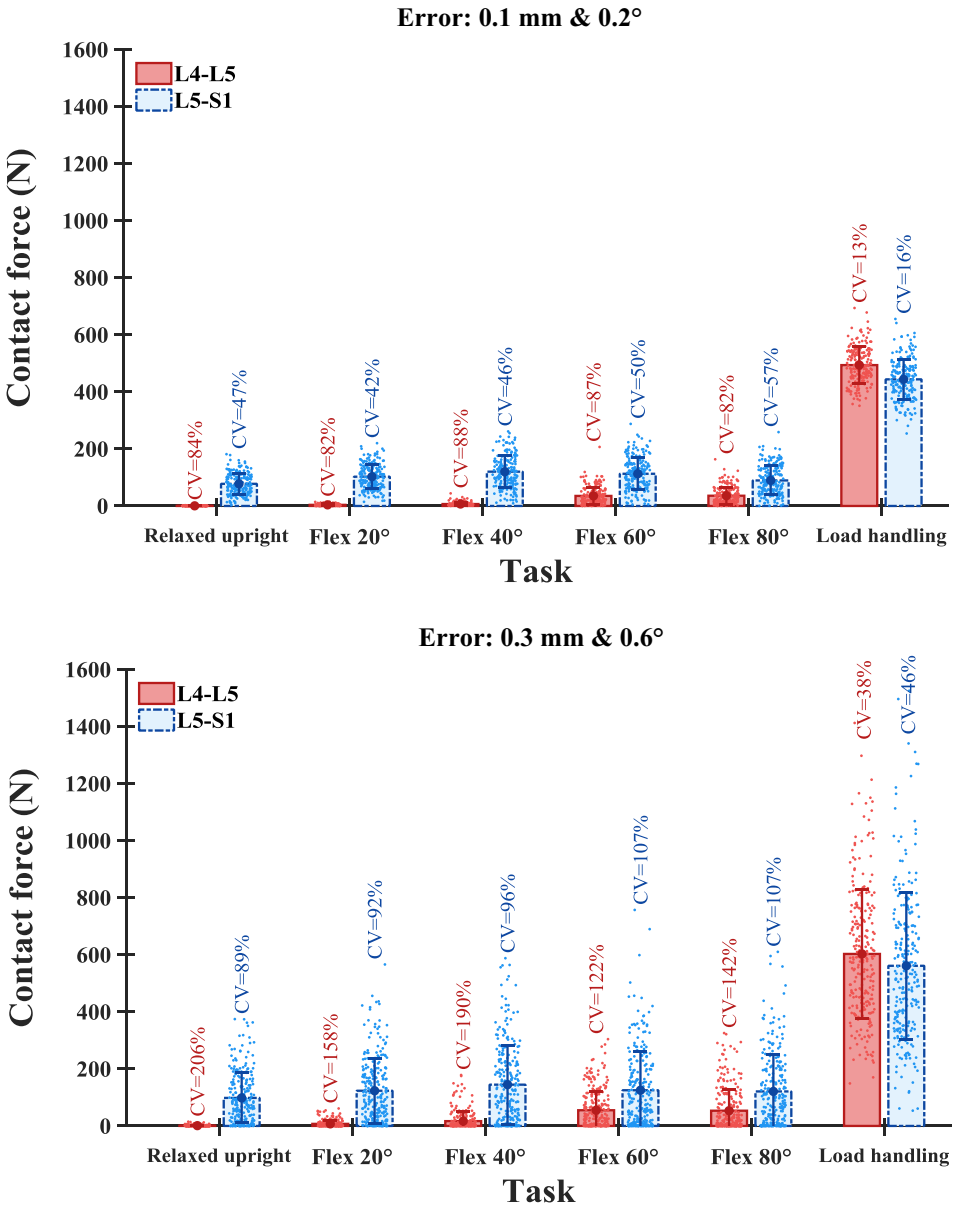

Fig. 6. Mean, standard deviation and coefficient of variation (CV) for the contact forces (sum of left and right contact forces) in L4-L5 and L5-S1 facet joints computed in the FE model in different tasks. The scatter dots (200 data points for each task) present the predicted ligament forces for various sensitivity simulations (0.1 mm & 0.2° and 0.3 mm & 0.6°).

not accurate enough to drive biomechanical models when estimating spinal loads.

4.1. Limitations

Sensitivity of the models to displacement errors depends also on the assumed joint stiffness in the translational and rotational directions; larger effects are expected in stiffer joints and directions despite identical variations in input displacements. For instance, intervertebral joints in the MS model are simulated as deformable beams with level-dependent linear shear-displacement response in accordance with a number of in vitro e.g., (Gardner-Morse and Stokes, 2004; Miller et al., 1986; Skrzypiec et al., 2012; Tencer et al., 1982) and detailed FE modeling (Schmidt et al., 2013; Weisse et al., 2012) studies. In accordance, MS models take linear force-displacement properties, albeit at different magnitudes, in shear directions (Arjmand and Shirazi-Adl, 2006a; Meng et al., 2015; Stokes and Gardner-Morse, 1995). As a result, and since our MS model is softer in shear than that of Meng et al. (2015), for instance, greater sensitivity to errors in image-based shear displacements is expected in the latter model.

Predictions of the present MS and FE models for IDP, muscle activity, FJFs, range of motion, and vertebral center of rotation under various loading conditions have however extensively been validated (Arjmand et al., 2009, 2010; Khoddam-Khorasani et al., 2018). Moreover, the effect of concurrent changes in the geometry of passive and active structures such as disc heights and cross-sectional areas on the sensitivity of the models were not investigated here as earlier works have reported the significant influence on results of alterations in the disc dimensions (Natarajan and Andersson, 1999; Zander et al., 2017). Models with shorter discs or with discs having greater cross-sectional areas may show greater sensitivity to the accuracy in measured displacements (Lu et al., 1996; Meijer et al., 2011; Niemeyer et al., 2012). Neverthe-

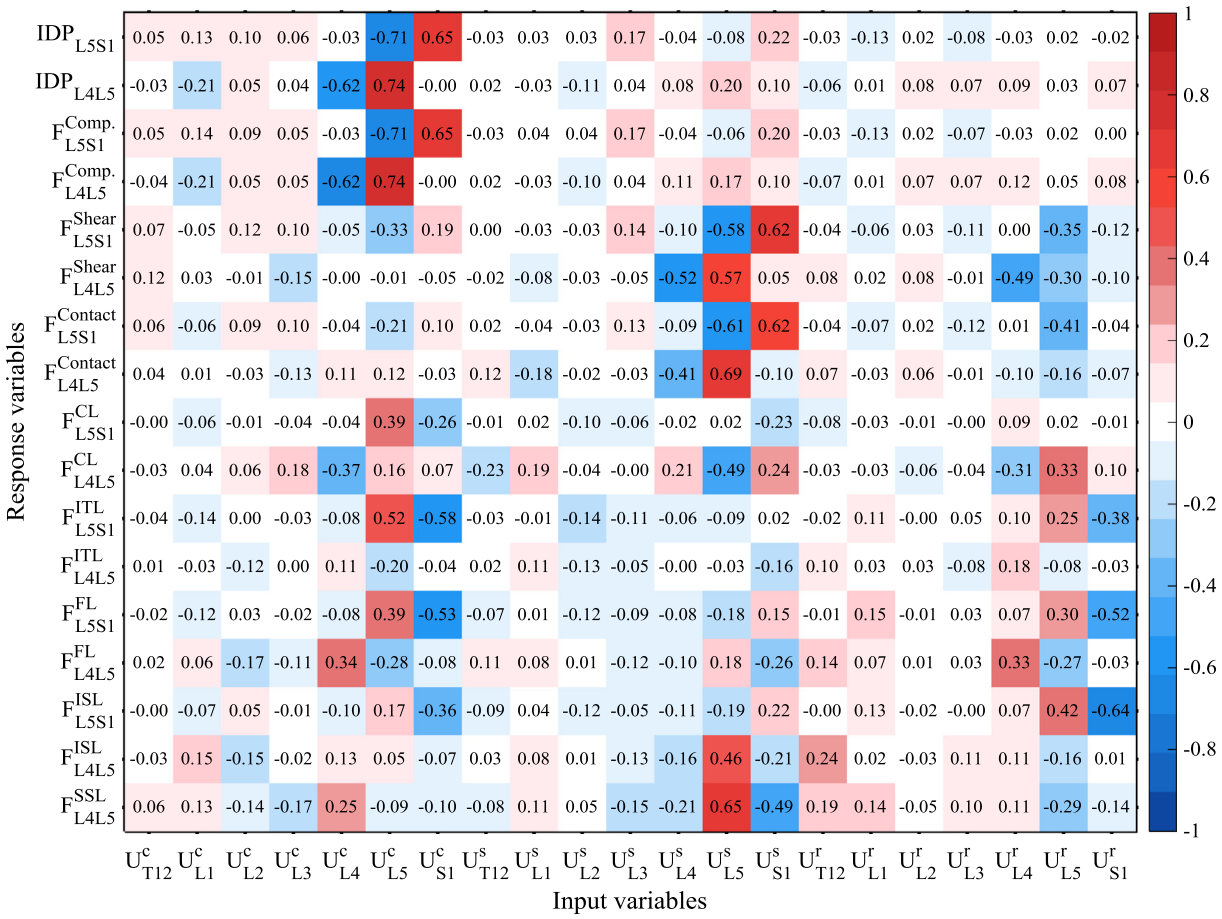

Fig. 7. Pearson correlation coefficient (r) for all input and select output variables in neutral upright posture in the FE model for the sensitivity analysis of 0.1 mm & 0.2°.

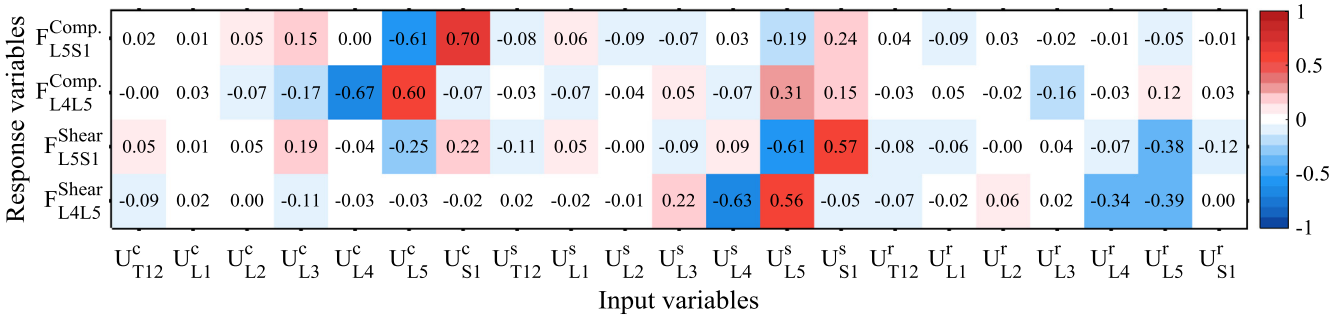

Fig. 8. Pearson correlation coefficient (r) for all input and select output variables in neutral upright postures in the MS model for the sensitivity analysis of 0.1 mm & 0.2°.

less, in view of the relatively large stiffness of motion segments especially under larger loads, it can be concluded that all spine models are particularly hypersensitive to errors in the measured translations. The extent of this sensitivity may, however, vary from a model to another. These observations are supported by the substantial sensitivity in computed contact mechanics in knee replacement systems under variations as small as ±0.1 mm or degree in input displacements (Fregly et al., 2008) to the extent that authors suggested the use of a combined force-displacement in place of a pure displacement-control approach. Finally, it is to be noted that a normal probability distribution in input (displacement errors) variations was assumed in the Monte Carlo analysis. Considering a different distribution would likely affect the predicted sensitivities, but not conclusions, in this study.

4.2. Analysis of results

Despite the rather small range of displacement errors considered in this study (SD = 0.1–0.3 mm and 0.2–0.6°), large effects on predictions of both models were found (Tables 1 and 2 and Figs. 2–6). In some instances, even tensile, rather than compressive, axial forces (Fig. 3) and posterior, rather than anterior, shear forces (Fig. 4) were predicted at different disc levels. We could expect even larger errors in the measurements of imaged-based vertebral displacements when considering the likely inter-rater or inter-method variabilities in identifying vertebral edges in these images. It is also to be noted that the absolute errors in the predicted IDPs, disc compression-shear forces, and FJFs generally grow in more demanding tasks (Tables 1 and 2 and Figs. 2–6; for

instance, see errors in the predicted FJFs in load handling tasks and in the predicted IDPs in flexion of 80°).

Validation of the full displacement-control spine models by comparing the predicted IDPs under some given tasks with the corresponding measured ones should also be taken with caution. This is due to marked effect of displacement errors on the predicted IDPs that reach as large even as the reported measured IDPs. For instance, while we predicted a SD of ~0.42 MPa (for a 0.3 mm error) in L4-L5 IDP in the relaxed upright posture (Table 1), (Wilke et al., 2001) measured the corresponding IDP in the same range at 0.43–0.5 MPa. For more demanding tasks the issue appears to slightly ease off but remains yet important; e.g., for load handling task, the predicted L4-L5 IDP showed a SD of 0.52 MPa that is about half the measured IDP at 1.0 MPa. Therefore, and at the current displacement error levels in imaging, full displacement-control models appear to be inadequate for the estimation of detailed internal joint loads. Moreover, when using full displacement-control models in which unique displacements are applied on entire vertebrae, the relative motion of posterior elements of a vertebra with respect to its anterior body is totally neglected. This becomes especially crucial when simulating tasks with large flexion (due to ligamentous forces) or extension (due to facet contact forces) trunk angles in which posterior elements displace distinctly from the anterior vertebral body (Shirazi-Adl, 1994a; Shirazi-Adl and Argoubi, 1994). Application of full displacement-control models is further questionable due to the radiation exposure in X-ray and CT machines (Aiyangar et al., 2014; Ochia et al., 2006). Due to the high acquisition time, using the risk-free upright MR machine to obtain vertebral kinematics is also limited to tasks that are not physically demanding (Meakin et al., 2009). Moreover, these approaches often provide limited spaces to measure real physiological activities with free unconstrained movements.

Since model predictions are found less sensitive to the errors in the measured vertebral rotations as compared to those in vertebral translations (Figs. 7–8 and supplementary materials 2 and 3), traditional models that use only vertebral rotations as input to drive models (Arjmand and Shirazi-Adl, 2006a; Cholewicki and McGill, 1996; Eskandari et al., 2017) appear hence more appropriate for the estimation of spinal loads. The accuracy of these combined displacement- and force-control models remain nevertheless, as expected, dependent on the optimization- or EMG-assisted approach used to estimate muscle forces. Despite large differences in the predicted muscle forces observed when comparing these techniques, predicted axial compressive forces are found comparable (Arjmand et al., 2009, 2010; Arjmand and Shirazi-Adl, 2006b; Mohammadi et al., 2015). The traditional models driven by segmental rotations, gravity and external loads are hence reliable to be used in occupational biomechanics.

In conclusion, any measurement technique with translational error $\geq$ 0.1 mm is not accurate enough to drive displacement-control models for the estimation of detailed internal joint loads. Moreover, when using displacement-control modeling, performing a comprehensive sensitivity analysis is essential in order to assess the reliability and sensitivity of predictions.

Acknowledgment

This work was supported by grants from Sharif University of Technology (Tehran, Iran). Assistance of Mr. P. Khoddam-Khorasani in the finite element analyses is gratefully acknowledged.

Conflict of interest statement

The authors state that there is no conflict of interest to report.

Appendix A. Supplementary material

Supplementary data to this article can be found online at https://doi.org/10.1016/j.jbiomech.2018.12.043.

References

Aiyangar, A.K., Zheng, L., Tashman, S., William, J.A., Xudong, Z., 2014. Capturing three-dimensional in vivo lumbar intervertebral joint kinematics using dynamic stereo-X-ray imaging. J. Biomech. Eng. 136, 011004.
Ali, A.H., Cowan, A.B., Gregory, J.S., Aspden, R.M., Meakin, J.R., 2012. The accuracy of active shape modelling and end-plate measurements for characterising the shape of the lumbar spine in the sagittal plane. Comput. Methods Biomech. Biomed. Eng. 15, 167–172.
Arjmand, N., Gagnon, D., Plamondon, A., Shirazi-Adl, A., Larivière, C., 2009. Comparison of trunk muscle forces and spinal loads estimated by two biomechanical models. Clin. Biomech. 24, 533–541.
Arjmand, N., Gagnon, D., Plamondon, A., Shirazi-Adl, A., Larivière, C., 2010. A comparative study of two trunk biomechanical models under symmetric and asymmetric loadings. J. Biomech. 43, 485–491.
Arjmand, N., Shirazi-Adl, A., 2005. Biomechanics of changes in lumbar posture in static lifting. Spine 30, 2637–2648.
Arjmand, N., Shirazi-Adl, A., 2006a. Model and in vivo studies on human trunk load partitioning and stability in isometric forward flexions. J. Biomech. 39, 510–521.
Arjmand, N., Shirazi-Adl, A., 2006b. Sensitivity of kinematics-based model predictions to optimization criteria in static lifting tasks. Med. Eng. Phys. 28, 504–514.
Breau, C., Shirazi-Adl, A., De Guise, J., 1991. Reconstruction of a human ligamentous lumbar spine using CT images - A three-dimensional finite element mesh generation. Ann. Biomed. Eng. 19, 291–302.
Cholewicki, J., McGill, S.M., 1996. Mechanical stability of the in vivo lumbar spine: implications for injury and chronic low back pain. Clin. Biomech. 11, 1–15.
Dehghan Hamani, I., Arjmand, N., Shirazi Adl, A., 2019. Subject-specific loads on the lumbar spine in detailed finite element models scaled and driven by radiography images. Int. J. Numerical Methods Biomed. Eng.
Dombrowski, M.E., Rynearson, B., LeVasseur, C., Adgate, Z., Donaldson, W.F., Lee, J.Y., Aiyangar, A., Anderst, W.J., 2018. ISSLS PRIZE IN BIOENGINEERING SCIENCE 2018: dynamic imaging of degenerative spondylolisthesis reveals mid-range dynamic lumbar instability not evident on static clinical radiographs. Eur. Spine J.: Off. Publ. Eur. Spine Soc. Eur. Spinal Deformity Soc. Eur. Sect. Cervical Spine Res. Soc. 27, 752–762.
Dreischarf, M., Shirazi-Adl, A., Arjmand, N., Rohlmann, A., Schmidt, H., 2016. Estimation of loads on human lumbar spine: a review of in vivo and computational model studies. J. Biomech. 49, 833–845.
El-Rich, M., Shirazi-Adl, A., Arjmand, N., 2004. Muscle activity, internal loads, and stability of the human spine in standing postures: combined model and in vivo studies. Spine 29, 2633–2642.
Eskandari, A., Arjmand, N., Shirazi-Adl, A., Farahmand, F., 2017. Subject-specific 2D/3D image registration and kinematics-driven musculoskeletal model of the spine. J. Biomech. 57, 18–26.
Fregly, B.J., Banks, S.A., D'Lima, D.D., Colwell Jr., C.W., 2008. Sensitivity of knee replacement contact calculations to kinematic measurement errors. J. Orthopaedic Res.: Off. Publ. Orthopaedic Res. Soc. 26, 1173–1179.
Frobin, W., Brinckmann, P., Leivseth, G., Biggemann, M., Reikerås, O., 1996. Precision measurement of segmental motion from flexion—extension radiographs of the lumbar spine. Clin. Biomech. 11, 457–465.
Gardner-Morse, M.G., Stokes, I.A.F., 2004. Structural behavior of human lumbar spinal motion segments. J. Biomech. 37, 205–212.
Khoddam-Khorasani, P., Arjmand, N., Shirazi-Adl, A., 2018. Trunk hybrid passive-active musculoskeletal modeling to determine the detailed T12–S1 response under in vivo loads. J. Ann. Biomed. Eng., 1–14
Lu, M.Y., Hutton, W.C., Gharpuray, V.M.J.S., 1996. Can variations in intervertebral disc height affect the mechanical function of the disc? Spine 21, 2208–2216.
Meakin, J.R., Gregory, J.S., Aspden, R.M., Smith, F.W., Gilbert, F.J., 2009. The intrinsic shape of the human lumbar spine in the supine, standing and sitting postures: characterization using an active shape model. J. Anat. 215, 206–211.
Meijer, G.J., Homminga, J., Veldhuizen, A.G., Verkerke, G.J., 2011. Influence of interpersonal geometrical variation on spinal motion segment stiffness: implications for patient-specific modeling. Spine 36, E929–E935.
Meng, X., Bruno, A.G., Cheng, B., Wang, W., Bouxsein, M.L., Anderson, D.E., 2015. Incorporating six degree-of-freedom intervertebral joint stiffness in a lumbar spine musculoskeletal model—method and performance in flexed postures. J. Biomech. Eng. 137.
Miller, J.A., Schultz, A.B., Warwick, D.N., Spencer, D.L., 1986. Mechanical properties of lumbar spine motion segments under large loads. J. Biomech. 19, 79–84.
Mohammadi, Y., Arjmand, N., Shirazi-Adl, A., 2015. Comparison of trunk muscle forces, spinal loads and stability estimated by one stability-and three EMG-assisted optimization approaches. Med. Eng. Phys. 37, 792–800.
Natarajan, R.N., Andersson, G.B., 1999. The influence of lumbar disc height and cross-sectional area on the mechanical response of the disc to physiologic loading. Spine 24, 1873.
Niemeyer, F., Wilke, H.-J., Schmidt, H., 2012. Geometry strongly influences the response of numerical models of the lumbar spine—a probabilistic finite element analysis. J. Biomech. 45, 1414–1423.

Ochia, R.S., Inoue, N., Renner, S.M., Lorenz, E.P., Lim, T.-H., Andersson, G.B., An, H.S.J. S., 2006. Three-dimensional in vivo measurement of lumbar spine segmental motion. Spine 31, 2073–2078.
Pearcy, M., Portek, I., Shepherd, J., 1984. Three-dimensional x-ray analysis of normal movement in the lumbar spine. Spine (Phila Pa 1976) 9, 294–297.
Reeves, N.P., Cholewicki, J., 2003. Modeling the human lumbar spine for assessing spinal loads, stability, and risk of injury. Crit. Rev. Biomed. Eng. 31, 73–139.
Schmidt, H., Bashkuev, M., Dreischarf, M., Rohlmann, A., Duda, G., Wilke, H.J., Shirazi-Adl, A., 2013. Computational biomechanics of a lumbar motion segment in pure and combined shear loads. J. Biomech. 46, 2513–2521.
Shirazi-Adl, A., 1994a. Analysis of role of bone compliance on mechanics of a lumbar motion segment. J. Biomech. Eng. 116, 408–412.
Shirazi-Adl, A., 1994b. Biomechanics of the lumbar spine in sagittal/lateral moments. Spine 19, 2407–2414.
Shirazi-Adl, A., Argoubi, M., 1994. Nonlinear poroelastic analysis of lumbar motion segments in prolonged compression postures. In: Proceedings of the 1994 International Mechanical Engineering Congress and Exposition. New York, NY, United States, Chicago, IL, USA.
Shirazi-Adl, S.A., Shrivastava, S.C., Ahmed, A.M.J.S., 1984. Stress analysis of the lumbar disc-body unit in compression. A three-dimensional nonlinear finite element study. Spine 9, 120–134.
Skrzypiec, D.M., Klein, A., Bishop, N.E., Stahmer, F., Puschel, K., Seidel, H., Morlock, M.M., Huber, G., 2012. Shear strength of the human lumbar spine. Clin. Biomech. (Bristol, Avon) 27, 646–651.
Stokes, I.A., Gardner-Morse, M., 1995. Lumbar spine maximum efforts and muscle recruitment patterns predicted by a model with multijoint muscles and joints with stiffness. J. Biomech. 28, 177–186.
Tencer, A., Ahmed, A., Burke, D.L., 1982. Some static mechanical properties of the lumbar intervertebral joint, intact and injured. J. Biomech. Eng. 104, 193–201.
Wang, S., Park, W.M., Kim, Y.H., Cha, T., Wood, K., Li, G., 2014. In vivo loads in the lumbar L3–4 disc during a weight lifting extension. Clin. Biomech. (Bristol, Avon) 29, 155–160.
Weisse, B., Aiyangar, A.K., Affolter, C., Gander, R., Terrasi, G.P., Ploeg, H., 2012. Determination of the translational and rotational stiffnesses of an L4–L5 functional spinal unit using a specimen-specific finite element model. J. Mech. Behav. Biomed. Mater. 13, 45–61.
Wilke, H.-J., Neef, P., Hinz, B., Seidel, H., Claes, L., 2001. Intradiscal pressure together with anthropometric data–a data set for the validation of models. Clin. Biomech. 16, S111–S126.
Zander, T., Dreischarf, M., Timm, A.-K., Baumann, W.W., Schmidt, H., 2017. Impact of material and morphological parameters on the mechanical response of the lumbar spine–a finite element sensitivity study. J. Biomech. 53, 185–190.
Zanjani-Pour, S., Meakin, J.R., Breen, A., Breen, A., 2018. Estimation of in vivo inter-vertebral loading during motion using fluoroscopic and magnetic resonance image informed finite element models. J. Biomech. 70, 134–139.
Zanjani-Pour, S., Winlove, C.P., Smith, C.W., Meakin, J.R., 2016. Image driven subject-specific finite element models of spinal biomechanics. J. Biomech. 49, 919–925.